



Contents lists available at ScienceDirect

Solid-State Electronics

journal homepage: [www.elsevier.com/locate/sse](http://www.elsevier.com/locate/sse)

# Infrared light emitting device with two color emission

Naresh C. Das

Army Research Laboratory, 2800 Powder Mill Rd., Adelphi, MD 20783, USA

## ARTICLE INFO

### Article history:

Received 1 February 2010

Received in revised form 2 June 2010

Accepted 9 June 2010

Available online xxx

The review of this paper was arranged by Prof. E. Calleja

### Keywords:

MWIR LEDs

LWIR LEDs

Interband cascade

Cryogenic operation

## ABSTRACT

We have designed and fabricated two-color infrared light emitting diode (LED) emitting in the wavelength regions of 3–4  $\mu\text{m}$  and 5–10  $\mu\text{m}$ . The interband cascade (IC) LED device was grown on n-type GaSb substrate and has 30 cascaded stages for the long-wave infrared (LWIR) and 15 cascaded stages for the mid-wave infrared (MWIR) emission bands. The two active regions are separated by a 0.5  $\mu\text{m}$  thick contact layer, which is used for biasing the two LEDs. Both room temperature and cryogenic temperature results show emission in the wavelength regions as designed.

Published by Elsevier Ltd.

## 1. Introduction

There exists a large demand for efficient, broad spectrum infrared light sources for various military and commercial sensor applications. For example, IR light emitting sources are the heart of the hardware-in-the-loop (HWIL) application for IR scene generation experiments [1]. In HWIL application infrared light sources like polysilicon resistor array and LED array are used to create an artificial battle field environments infrared scene which then projected to IR sensors to evaluate their performance. This process is also called as HWIL testing in synthetic environments. Because of considerable advantages in terms of cost, volume, long term reliability, and fast switching speed, IR LEDs are desirable for this and many other applications. Quantum cascade structures had great success as lasers in the infrared but have the problem of fast phonon relaxation, which limits their possible use as LEDs. Type-II Interband quantum cascade structures were proposed as a means to circumvent these fast phonon relaxation rates. Type-II Interband cascade (IC) electroluminescence in the 5–8  $\mu\text{m}$  spectral region from an LED structure was first reported by Yang et al. [2]. Type-II Interband cascade structures have the added advantages of carrier recycling and of emission either parallel or perpendicular to the surface. Recently, we reported the fabrication and operation of LED arrays in the 3–4  $\mu\text{m}$  and 8–10  $\mu\text{m}$  wavelength regions [3,4]. However, many biological and chemical sensor applications require efficient IR light sources emitting over broad spectral regions covering both MWIR and LWIR spectral

bands [5,6]. Another important application of two-color LEDs is in testing multi wavelength IR sensors in HWIL scene projection experiments. We present in this paper the performance of a single LED device emitting light in both the MWIR and LWIR spectral regions. Two wavelength bands of LED emission are carefully chosen to be below and above atmospheric spectral band (5–7  $\mu\text{m}$ ) where most of the IR sensors are used. Multi wavelength IR sensors can be evaluated using single LED device with multi wavelength emission.

## 2. Device fabrication

The IC LED structure was grown by molecular-beam epitaxy on an n-type GaSb substrate. After growing a 1.0  $\mu\text{m}$  thick p+ GaSb bottom contact layer, the LWIR IC LED structure was grown containing a 30 period active/injection region. Next, a 0.5  $\mu\text{m}$  thick p+ GaSb middle contact layer was grown followed by the MWIR IC LED structure containing a 15 period active/injection region. Finally a 1.4  $\mu\text{m}$  p+ GaSb top contact layer and grating host layer was grown. Each active/injection strain-compensated period includes an asymmetric  $\text{InAs}/\text{Ga}_{1-x}\text{In}_x\text{Sb}/\text{InAs}$  “W” quantum well preceded by an n-type digitally graded  $\text{InAs}/\text{AlSb}$  superlattice injector. The details of the band structure are presented in an earlier publication [3].

The LED fabrication process starts with reactive ion etching of a top grating which consists of a circular grating pattern with a 5  $\mu\text{m}$  pitch and 50% duty cycle (along the radial direction). The grating etch depth was 1.0  $\mu\text{m}$ . The grating structure is used to increase the detected signal which is due to the scattering of light out of

E-mail address: [naresh.das@us.army.mil](mailto:naresh.das@us.army.mil)

Report Documentation Page				Form Approved OMB No. 0704-0188	
Public reporting burden for the collection of information is estimated to average 1 hour per response, including the time for reviewing instructions, searching existing data sources, gathering and maintaining the data needed, and completing and reviewing the collection of information. Send comments regarding this burden estimate or any other aspect of this collection of information, including suggestions for reducing this burden, to Washington Headquarters Services, Directorate for Information Operations and Reports, 1215 Jefferson Davis Highway, Suite 1204, Arlington VA 22202-4302. Respondents should be aware that notwithstanding any other provision of law, no person shall be subject to a penalty for failing to comply with a collection of information if it does not display a currently valid OMB control number.					
1. REPORT DATE <b>09 JUN 2010</b>		2. REPORT TYPE		3. DATES COVERED <b>00-00-2010 to 00-00-2010</b>	
4. TITLE AND SUBTITLE <b>Infrared light emitting device with two color emission</b>				5a. CONTRACT NUMBER	
				5b. GRANT NUMBER	
				5c. PROGRAM ELEMENT NUMBER	
6. AUTHOR(S)				5d. PROJECT NUMBER	
				5e. TASK NUMBER	
				5f. WORK UNIT NUMBER	
7. PERFORMING ORGANIZATION NAME(S) AND ADDRESS(ES) <b>Army Research Laboratory, 2800 Powder Mill Rd, Adelphi, MD, 20783</b>				8. PERFORMING ORGANIZATION REPORT NUMBER	
9. SPONSORING/MONITORING AGENCY NAME(S) AND ADDRESS(ES)				10. SPONSOR/MONITOR'S ACRONYM(S)	
				11. SPONSOR/MONITOR'S REPORT NUMBER(S)	
12. DISTRIBUTION/AVAILABILITY STATEMENT <b>Approved for public release; distribution unlimited</b>					
13. SUPPLEMENTARY NOTES					
14. ABSTRACT <b>We have designed and fabricated two-color infrared light emitting diode (LED) emitting in the wavelength regions of 3?4 lm and 5?10 lm. The interband cascade (IC) LED device was grown on n-type GaSb substrate and has 30 cascaded stages for the long-wave infrared (LWIR) and 15 cascaded stages for the mid-wave infrared (MWIR) emission bands. The two active regions are separated by a 0.5 lm thick contact layer, which is used for biasing the two LEDs. Both room temperature and cryogenic temperature results show emission in the wavelength regions as designed.</b>					
15. SUBJECT TERMS					
16. SECURITY CLASSIFICATION OF:			17. LIMITATION OF ABSTRACT <b>Same as Report (SAR)</b>	18. NUMBER OF PAGES <b>3</b>	19a. NAME OF RESPONSIBLE PERSON
a. REPORT <b>unclassified</b>	b. ABSTRACT <b>unclassified</b>	c. THIS PAGE <b>unclassified</b>			

the mesa more efficiently, and is not of specific interest to the present study of two-color IR LED emission. Regions of the middle and bottom contact layers were exposed and individual  $100\ \mu\text{m} \times 100\ \mu\text{m}$  MWIR/LWIR LED mesas are isolated from other pixels in the array using a two mask photolithography process. The etch depths of the middle and bottom contact layers are 2.6 and  $4.5\ \mu\text{m}$ , respectively. Silicon nitride dielectric is deposited by the PECVD technique at  $250\ ^\circ\text{C}$ , and contact windows are opened in the dielectric on the top, middle, and bottom contact layers. Ti/Au metal contacts were then deposited for all three contact pads. A schematic diagram of the LED device's cross-section is shown in Fig. 1.

### 3. Results and discussion

In Fig. 2, we show the Fourier transform infrared (FTIR) emission curves for a single, two-color LED device at two temperatures. We used an FTIR spectrometer in single beam mode and an external HgCdTe detector to obtain the emission spectra. For the MWIR spectra we applied a positive bias to the top metal contact with the middle contact grounded. We applied a 40 mA pulsed current with a  $3\ \mu\text{s}$  pulse width and 50% duty cycle to obtain the spectra. For the LWIR spectra we applied a positive bias to the middle contact layer with the bottom contact layer grounded. Each spectrum was taken by subtracting background spectra measured with the device off. The MWIR and LWIR spectra for room temperature device operation peak at  $3.8$  and  $8\ \mu\text{m}$ , respectively. For cryogenic operation, the emission peaks shift to shorter wavelengths of  $3.2$  and  $7\ \mu\text{m}$  for the MWIR and LWIR devices, respectively. The emission spectrum of the LWIR device at 196 K mostly overlaps with the atmospheric absorption region of  $5\text{--}7\ \mu\text{m}$ . Hence we observed noise as well as low intensity in the LWIR spectra at 196 K.

The current–voltage (IV) curves at two different temperatures are shown in Fig. 3. As expected, the voltages across both devices are lower at room temperature (298 K) than at cryogenic temperatures. Moreover, the increase in voltage when reducing the temperature to cryogenic temperatures is higher for the LWIR device than for the MWIR device. This is consistent with significantly higher current leakage in the LWIR diode compared to the MWIR diode. Also the slopes of the IV curves at lower current are different for the two devices implying significantly lower leakage current for the MWIR device at both measurement temperatures. The increase in voltage drop at cryogenic temperatures may be due the reduction in Auger recombination process [7].

Light was collected and collimated by a 2-in.-aperture lens with a focal length of 2-in. A 1-in. focal length lens was used to focus the light onto a HgCdTe detector. We observed maximum light output for an injection current of pulse width  $3\ \mu\text{s}$  and 50% duty cycle. Hence these parameters were fixed at those values for subsequent measurements with different injection currents. We have measured and found that the LED light emission has a Lambertian angular distribution. Hence, required corrections due to emission in a  $2\pi$  steradian solid angle and reflection from lens surfaces were

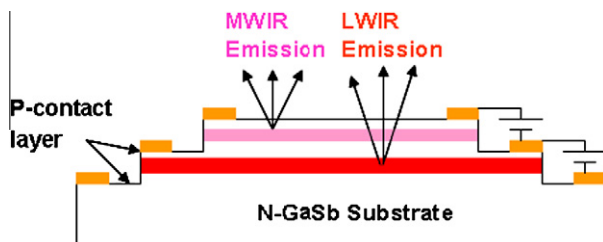


Fig. 1. Schematic diagram of LED structure with two IC stages separated by a contact layer.

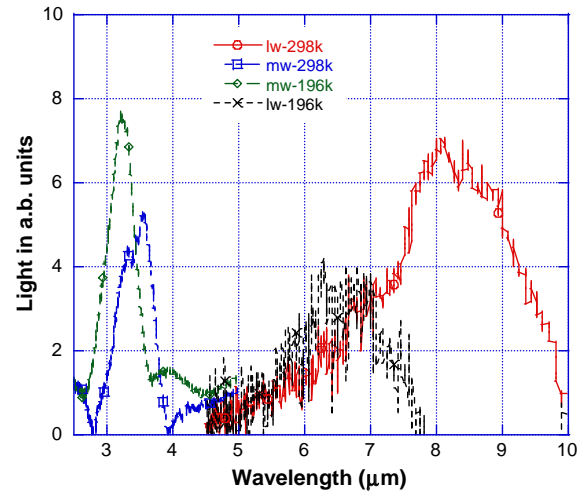


Fig. 2. Infrared spectra of MWIR and LWIR devices at two temperatures.

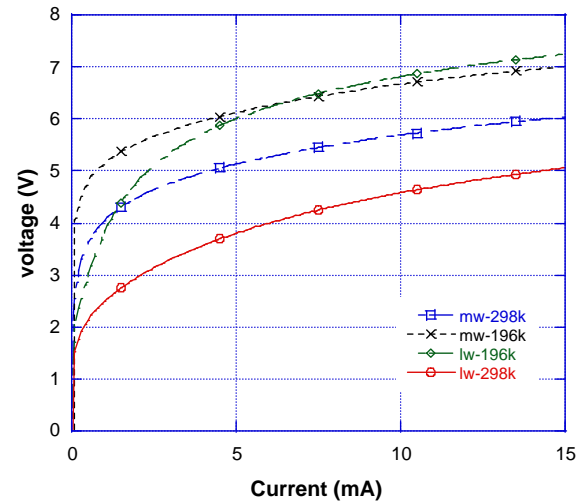


Fig. 3. Current versus voltage curves for LWIR and MWIR devices at room temperatures.

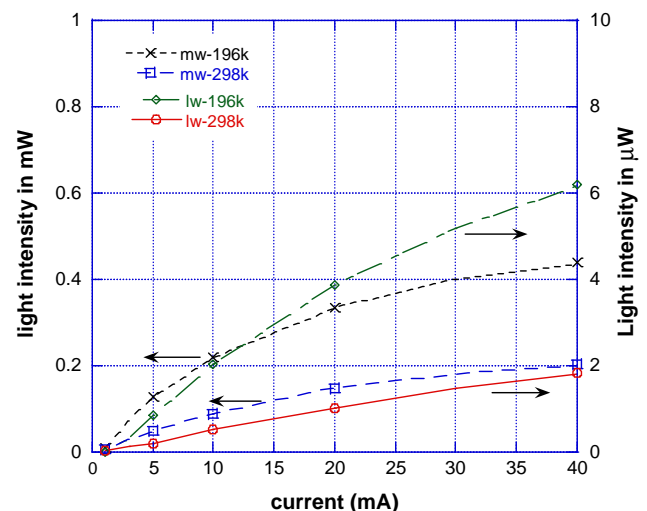


Fig. 4. Optical power versus current of the MWIR and LWIR devices.

made to convert the detector lock-in signal to a total output power. In Fig. 4, we present optical output power versus LED injection current (LI) for both the MWIR and LWIR devices at two temperatures. The total output power increases with injection current and attains saturation at higher current values. This can be attributed to more thermal leakage and other possible non-radiative carrier recombination processes that are enhanced at higher active region temperatures [8]. A large increase in light intensity ( $\sim$ doubling) is observed by cooling the device from room temperature to 196 K as the LED becomes progressively a more idealized type II heterojunction emitter. Compared to the MWIR device, the LWIR device experiences a more dramatic increase in light intensity at low temperature. This may also be due to the fact that at room temperature non-radiative recombination processes have an enhanced effect on the LWIR device, which has a significantly lower band-to-band transition energy compared to the MWIR device. We also observed saturation of LI curves at lower currents for the MWIR device compared to the LWIR device. The optical power output is higher for the MWIR device (approaching 1 mW) compared to the LWIR device (a few  $\mu$ W). As is evident from Fig. 3, the increase in voltage across the LWIR device at cryogenic temperatures is higher than that of the MWIR device. Likewise, we observed a higher increase in output power for the LWIR device (Fig. 4) compared to the MWIR device.

The MWIR IC structure is placed on top of the LWIR IC structure because the MWIR region is transparent to light from the LWIR layer, whereas the reverse is not true. The peak emission wavelengths for MWIR and LWIR devices at room temperature agree well with the design wavelengths of 3.8 and 8  $\mu$ m, respectively. At low temperatures, the peak emission wavelength shifts to shorter wavelength due to the increase of bandgap values [7]. The peak power of the LWIR spectrum at 196 K is lower than that at room temperature. This may be due to the fact that the plotted signal (Fig. 2) is obtained using background subtraction from the relatively low intensity LED emission superimposed on the large atmospheric absorption background signal. We used rapid scan FTIR equipment for obtaining LED spectra and hence could not subtract for each individual spectral bands. However we believe if a step scan FTIR is used it may be possible to accurately determine the effect of background signal for atmospheric absorption window in LWIR spectra. For top IC region MWIR device, the room temperature spectra range between 3 and 5  $\mu$ m. Similarly for LWIR bottom IC region device the room temperature spectra range is between 6 and 9  $\mu$ m. Hence by suitable bias of either top or bottom IC region, one can get either MWIR or LWIR light emission respectively. Also by applying ground bias to bottom of the LWIR IC region and positive bias to top MWIR IC region, one can get simultaneous MWIR and LWIR emission (not shown here). This simultaneous two color emission is useful for many sensor applications which require light source with broad emission spectra. As expected, the turn-on voltage of the LWIR device is less than that of the MWIR device as it depends on the energy of photon emission. For both devices, the voltage drops increase considerably with a temperature reduction indicating a decrease of some parasitic processes with decreasing temperature [9]. The optical output power characteristics from IC LED devices depend on many factors such as design and growth

parameters, processing techniques, device temperature, carrier relaxation mechanisms, and radiative recombination [10] phenomena. The details of the observed electroluminescence depend upon the competition between these processes. The injection current values corresponding to peak power at different temperatures are characteristics of the QW structure and device size. For higher injection currents above the peak emission value, various non-radiative processes including phonon relaxation processes become dominant [11] and optical power decreases. The large increase in optical power at cryogenic temperature (Fig. 4) may be due to a reduction in auger recombination process at lower temperatures [12,13].

In summary, we have shown here two-color IR emissions from a single device with independent biasing conditions. We have shown two wavelength bands of LED emission, but in principle multi wavelength IR emission is possible by appropriate design of the multiple IC epi structures. Such a device could be used in many biological and chemical sensor applications which require light sources with broad emission spectra.

### Acknowledgments

We thank Richard P. Leavitt and F. Towner of Maxion Technologies, Inc. for assistance with the epitaxial layer design and growth respectively.

### References

- [1] Brett Beasley D, Saylor DA, Bufford J. Overview of dynamic scene projectors at the US Army aviation and missile command. *Proc SPIE* 2002;4717:136.
- [2] Yang RQ, Lin C-H, Murry SJ, Pei SS, Liu HC, Buchanan M, et al. Interband cascade light emitting diodes in the 5–8  $\mu$ m spectrum region. *Appl Phys Lett* 1997;70:2013.
- [3] Das NC, Olver K, Towner F, Simonis G, Shen H. Infrared (3.8  $\mu$ m) interband cascade LED array with record high efficiency. *Appl Phys Lett* 2005;87:041105.
- [4] Das NC, Bradshaw J, Towner F, Leavitt R. Long-wave (10 micron) infrared light emitting diode device performance. *Solid State Electron* 2008;52:1821.
- [5] Hassinen I, Hiltunen J, Takala T. Reflectance spectrophotometric monitoring of the isolated perfused heart as a method of measuring the oxidation–reduction state of cytochromes and oxygenation of myoglobin. *Cardiovasc Res* 1981;15:86.
- [6] Hoang Shi-Hung, Horng Gor-Don, Chiang Chen-Yu, Ko Cheng-Hao, Lo Yi-Chung, Chen Ching-lue, et al. A novel measurement device for SAW chemical sensors with FT-IR spectro-microscopic analytical capability. *Tamkang J Sci Eng* 2005;8(1):63.
- [7] Y. Horikoshi. Semiconductors and semimetals. In: Tsang WT, editor. vol. 22C. New York: Academic; 1985 [chapter 3].
- [8] Pidgeon CR, Ciesla CM, Murnin BN. Suppression of non-radiative processes in semiconductor mid-infrared emitters and detectors. *Prog Quant Electron* 1998;21:361.
- [9] Popov AA, Shestnev VV, Yakovlev YP, Baranov AN, Alibert C. Powerful mid-infrared light emitting diodes for pollution monitoring. *Electron Lett* 1997;33:86.
- [10] Meyer JR, Hoffman CA, Bartoli FJ, Ram Mohan LR. Type II quantum well lasers for the mid infrared. *Appl Phys Lett* 1995;67:757.
- [11] Stringfellow GB, Craford MG, editors. Semiconductors and Semimetals: High Brightness LED, vol. 48. New York: Academic; 1997. p. 469.
- [12] Krier A, Gao HH, Shestnev VV, Yakovlev Y. Suppression of non-radiative processes in semiconductor mid-infrared emitters and detectors. *J Appl Phys* 1999;D 32:3117.
- [13] Smith DL, Mailhoit CM. Proposal for strained type II superlattice infrared detectors. *J Appl Phys* 1987;62:2545.